Rapeseed oil-based rigid polyisocyanurate foams modified with nanoparticles of various type*)

Ugis Cabulis[1),)], Irina Sevastyanova[1)], Jānis Andersons[2)], Ilze Beverte[2)]**

DOI: dx.doi.org/10.14314/polimery.2014.207

Abstract: Polyisocyanurate foams have been developed using a polyol system partially derived from rapeseed oil (RO). The effect of nanofillers with iso-dimensional geometry (zinc oxide), nanofibers (carbon nanotubes), and nanoplatelets (organically modified montmorillonite) on stiffness and strength of the foams has been studied. It was demonstrated that the tensile properties of the filled foams are enhanced by roughly the same proportion as the stiffness and strength of monolithic filled polymers.

Keywords: polyisocyanurate foams, rapeseed oil, monolithic polymer, nanofillers, compression, tension, stiffness, strength.

Pianki poliizocyjanurowe z udziałem poliolu z oleju rzepakowego modyfikowane różnego typu nanocząstkami

Streszczenie: Wytworzono pianki poliizocyjanurowe, stosując układ polioli pochodzących z oleju rzepakowego (RO). Badano wpływ nanonapełniaczy o geometrii sferycznej (tlenek cynku), nanowłókien (nanorurki węglowe) oraz nanopłytek (organicznie modyfikowany montmorylonit) na sztywność i wytrzymałość pianek poliizocyjanurowych. Stwierdzono poprawę właściwości wytrzymałościowych napełnionych pianek, porównywalną z poprawą sztywności i wytrzymałości napełnionych polimerów monolitycznych.

Słowa kluczowe: pianka polizocyjanurowa, olej rzepakowy, polimer monolityczny, nanonapełniacze, ściskanie, rozciąganie, sztywność, wytrzymałość.

Rigid polyurethane (PUR) and polyisocyanurate (PIR) foams are among the most important insulating materials currently used in the construction industry and are the principal insulation materials applied in the global appliances industry. Presently the primary raw materials used for the production of polyurethanes (including PUR and PIR foams) are products of petrochemical origin. But petroleum reserves are dwindling and, consequently, the prices of fuel and petrochemical raw materials are becoming increasingly unstable. The synthesis of polymers from renewable resources has been investigated by leading research teams from different countries [1]. Bio-based raw materials represent an abundant, renewable, non-food competitive, and low cost resource that could play an alternative role to petrochemical resources.

The first aim of the presented research is to use rapeseed oil (RO) as a raw material for production of bio-based PIR foams. The attention is focused on production of RO PIR bio-based foams using an innovative, sustainable synthetic process with reduced energy consumption [2].

Using the biopolymers as a matrix, a further step is to reinforce the bio-based polymer matrix with nano-size fillers to enhance its mechanical properties. Adding nanoparticles to foams has the potential to increase their strength and stiffness without compromising the advantages of light weight. Nanoparticles in a polymer matrix are known to serve a dual purpose: they act as foaming nucleation sites and also reinforce foam cell struts [3]. Three major types of nano-particles are discerned based on the number of dimensions in the nanometer range [4]:

— iso-dimensional nano-particles have all dimensions in the nanometer scale,

— nanofibers have two dimensions in the nanometer range,

— nanoplatelets have only one nanometer-scale dimension.

The type of nanofiller, as well as its chemical composition, affects the properties of the filled foams. Significantly higher gain in high-density PUR foam properties is reported for nanofiber-filled foams than for iso-dimen-

---

[1)] Latvian State Institute of Wood Chemistry, Dzerbenes 27, LV-1006, Riga, Latvia.

[2)] University of Latvia, Institute of Polymer Mechanics, Aizkraukles 23, LV-1006, Riga, Latvia.

[*)] Material contained in this article was presented on the 3rd Workshop on Green Chemistry and Nanotechnologies in Polymer Chemistry, 24—26 September, Cracow, Poland.

[**)] Author for correspondence; e-mail: cabulis@edi.lv sional oxide filler, with nanoplatelet reinforcement yielding intermediate results [5].

The second aim of the current study is determination of the effect of filler type on stiffness and strength of low-density foams. Iso-dimensional zinc oxide (ZnO) nanoparticles, carbon nanotubes (CNT), and organically modified montmorillonite (MMT) nanoplatelets are considered as fillers.

EXPERIMENTAL PART

Materials

Polyols on the basis of renewable natural oils, suitable for obtaining PUR and/or PIR, can be produced with different methods. Most often the esterification or epoxidation of oils are applied. In the present research polyol obtained by amidization of rapeseed oil (RO) with diethanolamine was used (temperature was 140 °C, as a catalyst was applied zinc acetate and the RO/diethanolamine molar ratio was 2.9/1.0). RO was obtained from the company Iecavnieks (Latvia). Firstly, optimum synthesis conditions of polyols suitable for obtaining PUR were determined. The synthesis process was monitored by determining changes in diethanolamine conversion degree (acid value and NH value).

The typical formulations of polyol component used in this study contain polyols from RO, and a higher functional polyether polyol based on sorbitol Lupranol 3422 from BASF (it contains only secondary hydroxyl groups, OH Number 490 mg KOH/g). As additives, surfactant NIAX Silicone L6915LV, from Momentive Performance Materials, and catalyst Polycat 5 from Air Products were used. Tris-chloropropyl phosphate (TCPP), used as a flame retardant, was supplied by Albemarle and as blowing agents, mix of water and cyclo-pentane were applied. As an isocyanate, polymeric diphenylmethane diisocyanate i.e. IsoPMDI 92140 supplied by BASF was used.

Three different nanoparticles have been used as fillers:

— iso-dimensional nanoparticles — zinc oxide Zano20 (produced by Umicore Zinc Chemicals) with the average size of ca. 30 nm;

— nanotubes — NC7000 (produced by Nanocyl) with average diameter of 9.5 nm and average length of 1.5 μm according to manufacturer's datasheet;

— nanoplatelets — organically modified montmorillonite (MMT) Cloisite®30B (produced by Southern Clay Products, Inc.) which is a purified natural MMT modified by methyl tallow bis-2-hydroxyethyl ammonium with a concentration of 90 meq/100 g clay.

Production of foams and monolithic polymers

PIR samples were obtained by mechanical mixing of appropriate amounts of IsoPMDI 92140 and the polyol system (polyols, surfactant, catalysts and blowing agent) for 10—15 s. The unreacted mixture was poured into a plastic mold (20 × 30 × 10 cm) for free foaming. The polymerization reaction took place at the room temperature.

To produce polymer nanocomposites, the nanoparticles were added to RO polyol at 1 wt % loading and dispersed by Ultrasonic Cell Crusher Model Sonic 650W (produced by MRC Scientific Instruments), with the capacity up to 0.6 dm^3/h, ultrasonic frequency 20—25 kHz and maximum power 650 W. The processing time was 1 h. Upon dispersion, filled foams were produced as described above. The fillers were added into a RO polyol foam formulation that provides density of neat foam $\rho_0 \approx 35$ kg/m^3.

For characterization of the mechanical properties of monolithic polymers, the mixture was poured into plastic ampules of ca. 15 mm inner diameter and 80 mm length. The ampules were centrifuged for 15 min at 5500 rpm by EBA20 centrifuge (produced by Hettich Zentrifugen) to eliminate bubbles.

Methods of mechanical testing

Compression of foams

The methodology of the compression tests followed that developed in [6]. Specimens where cut from slices of the foam blocks in the rise direction of the foams. Rectangular specimens of dimensions 40 × 20 × 20 mm (specimen with height to width ratio equal to 2) were tested for compression in the foam rise direction at the rate of 4 mm/min (10 %/min). Displacement parallel to the action line of external force was measured with a clip-on extensometer MTS 634.25F-24, base 8 mm. The deadweight of the extensometer was balanced by levers. Thin Teflon films were put between the top and bottom ends of specimens and the plates of the testing machine to reduce the friction.

Typical stress-strain diagrams of neat foams of ca. 35 kg/m^3 density and foams of the same formulation but filled by nanoparticles at 1 wt % loading are shown in Fig. 1a. A beneficial effect of filling on the foam stiffness and strength is clearly discerned.

Tension of foams

Specimens where cut from slices of the foam blocks in the transverse direction (i.e. normal to the rise direction of the foams). The specimens for tension tests had a dog-bone shape, with a rectangular test section of 85 mm length, 22 mm width and 20 mm thickness. An extensometer with 50 mm base length was used for strain measurement in the loading direction. For gripping, metallic plates with hooks were glued to the ends of the specimens. Chain elements provide alignment of the sample's axis with the action line of external force (see Fig. 2), thus eliminating bending and ensuring pure tension in the test

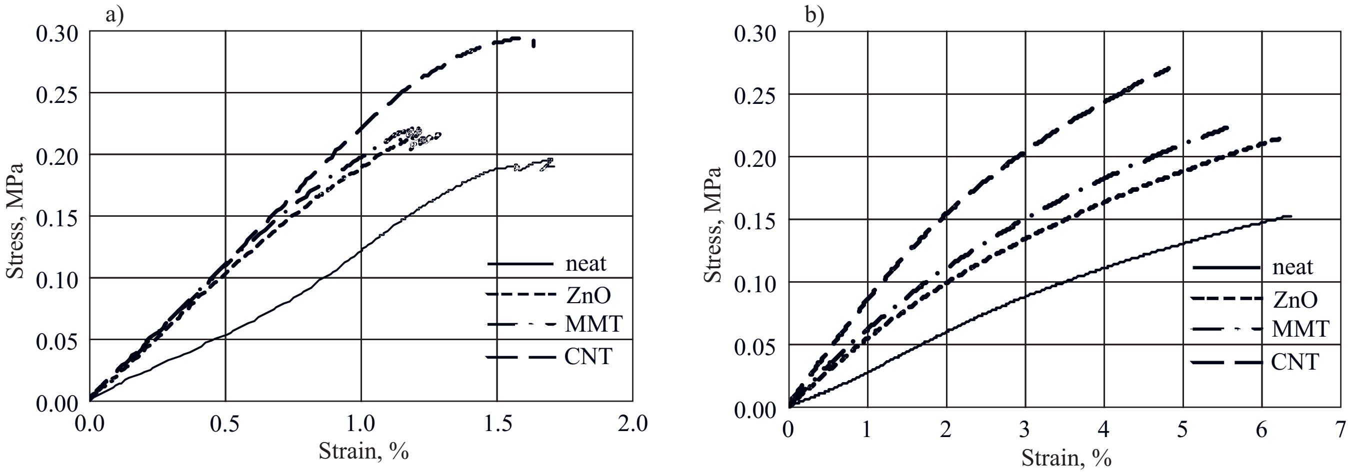

Fig. 1. Typical stress-strain diagrams of neat and filled at 1 wt % foams in compression along the foam rise direction (a) and in the transverse tension test (b)

section. Tensile tests were carried out by stroke control, at the displacement rate of 8 mm/min.

Fig. 1b illustrates the effect of fillers on the transverse tensile response of foams produced according to the formulation leading to ca. 35 kg/m^3 density of neat foams. Both stiffness and strength are enhanced by the presence of a filler, while the limit strain is slightly reduced, as in the case of compression shown in Fig. 1a.

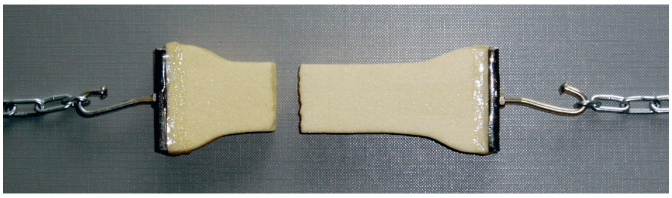

Fig. 2. Foam specimen with fixtures for tension tests

Compression and tension of monolithic polymers

The solid polymer samples were removed from ampules upon setting of the polymer. Specimens for compression test were made as cylinders of height 28 mm and diameter 14 mm. The longitudinal displacement was determined on the base of 8 mm and the transversal one — on the diameter. Compression tests were carried out at the strain rate of 1.5 %/min. Young's modulus and Poisson's ratio were determined from the initial, linear part of the stress-strain diagram.

For tension tests, cylindrical dog-bone shaped tension specimens were manufactured by turning. The length of the test section of the specimens amounted to ca. 28 mm and diameter to 5.5 mm. Specimen ends were glued into tubular aluminum tabs. Tensile tests were carried out by stroke control with the displacement rate of 1 mm/min.

For both, neat and filled polymers, an initial linear stress-strain response was observed, followed by yielding and a nonlinear deformation stage with strain-softening until the failure, in agreement with the results reported in [7] for PUR. Young's modulus was determined from the initial, linear part of the stress-strain diagram, while the maximum stress attained during test was taken as the strength [7].

RESULTS AND DISCUSSION

RO polyol and PIR foam properties

The obtained RO polyol is characterized by the following parameters: hydroxyl value 400 ± 5 mg KOH/g, acid value < 3 mg KOH/g, density 0.976 ± 0.001 g/cm^3, viscosity 825 ± 5 mPa · s, water content < 0.1 %. The obtained polyol is commercially prospective for production of rigid PUR and especially PIR foams.

The PIR foams obtained from IsoPMDI 92140 and polyol system have the following characteristics: isocyanate index 160, the content of RO polyol in the polyol system 50 %, the content of RO as a renewable raw material in the end product (ready PIR foams) 17 %, volume ratio of polyol component/IsoPMDI 92140 = 1/1.

Mechanical properties

Monolithic polymers

Mean values and standard deviations of Young's modulus and the tensile strength of monolithic polymers, both plain and filled at 1 wt %, are presented in Table 1. It is seen that all the nanofillers provide roughly equal increase in strength of ca. 11 % in comparison with neat PIR. Reinforcement efficiency for stiffness appears to depend on filler geometry, ranging from 6 % gain in Young's modulus in the case of iso-dimensional ZnO nanofiller to 11 % and 14 % gain for MMT and CNT, respectively. Such an effect of the shape of filler particles is expected, as an increase in the aspect ratio of reinforcement is known to result in higher composite stiffness.

T a b l e 1. Strength and Young's modulus of neat (E_p) and filled at 1 wt % (E_{fp}) monolithic polymers in the tension test

Filler	—	ZnO	CNT	MMT
E_p, MPa	2300 ± 180			
E_{fp}, MPa		2430 ± 82	2620 ± 65	2560 ± 215
Strength, MPa	58.5 ± 6.1	65.4 ± 2.7	64.9 ± 1.5	65.1 ± 2.9

Specifically, the relative stiffness gain for PIR filled by MMT amounted to $E_{fp}/E_p = 1.11$ according to the experimentally obtained Young's moduli of neat (E_p) and filled (E_{fp}) polymers reported in Table 1. A theoretical model of elastic constants of a composite reinforced with plate-like filler particles has been derived and applied to MMT-filled PUR in [8]. Fig. 7 of [8] provides the value of $E_{fp}/E_p \approx 1.1$ for 1 wt % loading of well exfoliated, randomly orientated MMT platelets in a composite. Considering PIR polymer as not considerably differing from PUR polymer, such a close agreement of the experimental data and theoretical prediction suggests a good level of MMT exfoliation in PIR achieved by ultrasonification.

In compression, the samples of neat polymer acquired the shape of a barrel without fracturing, stiffness 2318 ± 172 MPa and Poisson's ratio $\nu = 0.40 \pm 0.03$. The presence of the considered fillers did not appreciably affect the polymer density which amounted to ca. 1210 kg/m^3.

Stiffness of foams

The stiffness of foams depends on foam density, morphology, and the stiffness of the solid cell wall and strut material. Simple relations between mechanical properties of foams have been derived and presented in e.g. [9—11]. Young's modulus (E_f) of foam is related to strut stiffness (E_s) and density of foam and polymer (i.e. strut material), ρ_f and ρ_s, respectively, as follows:

$$E_f = C\left(\frac{\rho_f}{\rho_s}\right)^n E_s \qquad (1)$$

where: C, n — constants that reflect cell morphology.

Theoretical estimates of the exponent of eq. (1) have been derived for foams with uniform cells modeled as a network of cubes with equal edges, obtaining $n = 2$ for open cell and n approaching 1 for closed cell foams [11].

Stiffness in the foam rise direction, determined by compression tests, is shown in Fig. 3 as a function of the apparent foam density. It can be concluded that the compressive stiffness of the RO polyol-based foam is practically equal to the petrochemical foam stiffness [12] in the foam density range between 35 and 75 kg/m^3. It is seen that the experimental data can be reasonably well approximated by eq. (1), plotted by a solid line in Fig. 3. The best-fit value of the exponent n amounted to 1.3 and $C = 0.45$.

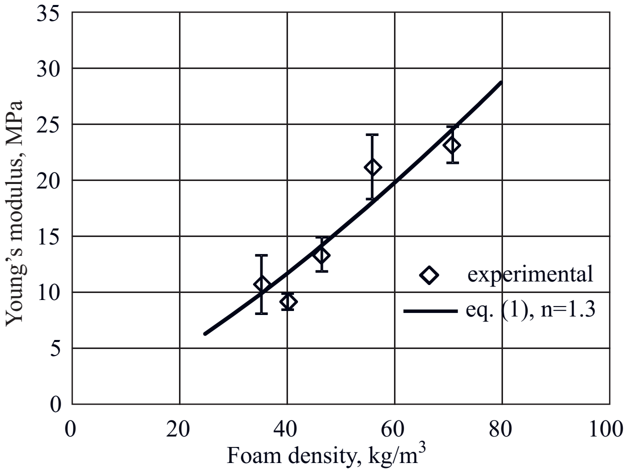

Fig. 3. Young's modulus in compression in the rise direction of neat foams as a function of the apparent foam density

Power-law dependence of stiffness on density given by eq. (1) for the same RO-based PIR foams has been demonstrated to hold also for the transverse direction (normal to the foam rise direction) [13], albeit with different values of constants.

As a first approximation, stiffness of the filled, composite foams (E_{cf}), can be predicted by the scaling relation given by eq. (1), allowing for the composite strut stiffness. Specifically, upon substituting foam density and polymer stiffness in eq. (1) by the respective quantities of filled foams and struts (ρ_{cf} and E_{cs}, respectively), we obtain:

$$E_{cf} = C\left(\frac{\rho_{cf}}{\rho_{cs}}\right)^n E_{cs} \qquad (2)$$

The experimental Young's modulus of filled foams is plotted in Fig. 4 as a function of the value predicted accor-

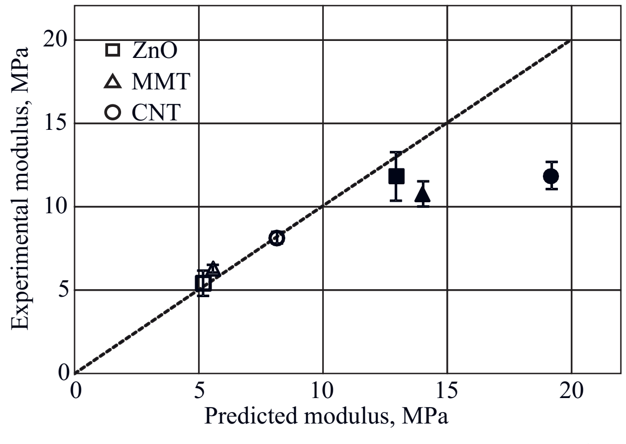

Fig. 4. Experimental Young's modulus in the rise direction (filled markers, compression) and transverse direction (open markers, tension) versus the prediction by eq. (2) for filled foams with 1 wt % loading of nanoparticles; dashed line corresponds to perfect agreement of prediction and test results

ding to eq. (2). An implicit assumption is made that nanofilling, while affecting the foam density, does not significantly alter the foam morphology at a given density compared to that of neat foams. This permits to use the values of parameters *C* and *n* established from eq. (1) for neat foam compression tests for compressive stiffness prediction of filled foams (shown by filled markers in Fig. 4), and those obtained from neat foam tensile test results — for prediction of tensile stiffness of filled foams (open markers). The same values of Young's modulus for filled polymer from Table 1 were used in both cases. The slope of the dashed line in Fig. 4 is equal to 1 what corresponds to equal experimental and predicted stiffness.

Due to anisotropy of the foams, stiffness in the rise direction exceeds that in the transverse direction both for neat (cf. Fig. 3 and the data in [13]) and filled foams, Fig. 4. It is seen that the highest foam stiffness in transverse tension is achieved using CNT, the least effective reinforcement is provided by ZnO, and only a slightly better effect is achieved by using MMT. By contrast, no discernible effect of nanofiller shape on the foam stiffness in compression in the rise direction is observed. The accuracy of prediction by eq. (2) is reasonably good, apart from the case of compressive stiffness of CNT-filled foams, which is overestimated by ca. 50 %.

Note that the stiffness of rigid PIR foams can be considered as equal in tension and compression only at low strains $|\varepsilon| < 0.3$ % according to [11]. In the strain regions of practical importance $|\varepsilon| > 1.0$ %, the stiffness in tension is by 10—30 % higher than in compression [11].

Strength of foams

Compressive strength of neat polymer foams in the rise direction versus apparent foam density is plotted in Fig. 5. It can be concluded that the compressive strength of the RO polyol-based foam is by about 25 % smaller than the petrochemical foam strength [12] in the foam density range between 35 and 75 kg/m^3.

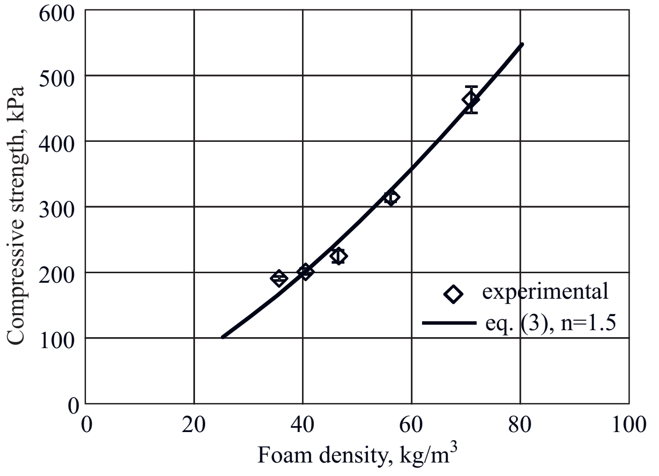

Fig. 5. Compressive strength in the rise direction of neat foams as a function of the apparent foam density

In the case of plastic collapse, the compressive strength is related to the foam density and yield strength (σ_{ys}) of the strut material as follows [9, 10]:

$$\sigma_f = C\left(\frac{\rho_f}{\rho_s}\right)^n \sigma_{ys} \tag{3}$$

The theoretical value of the exponent *n* is 3/2. Although strut strength may differ from that of a standard size specimen due to, e.g. the scale effect of strength or differences in morphology [14], the strut material strength as obtained from macroscopic specimen tests is usually used in eq. (3) [9, 10]. Employing the maximum stress sustained by the monolithic polymer reported in Table 1 as an estimate of σ_{ys}, approximation of the strength data of RO polyol-based PIR foams using eq. (3), shown in Fig. 5 by a solid line, produced the empirical estimate of *n* close to 1.5 and *C* = 0.49. For filled foams, eq. (3) is modified by replacing the neat foam density and polymer strength by those of the filled foams and polymer:

$$\sigma_{cf} = C\left(\frac{\rho_{cf}}{\rho_{cs}}\right)^n \sigma_{cys} \tag{4}$$

Having determined eq. (3) parameters, the theoretical compressive strength of filled foams is predicted by eq. (4) using the strength data of filled polymer foams presented in Table 1. The measured foam strength is plotted versus the predicted one in Fig. 6 by solid markers.

The transverse tensile strength of the neat RO polyol-based PIR foams considered here has been reported in [15] and shown to follow the power-law dependence on foam density given by eq. (3), albeit with different parameter values. Using eq. (3) parameters determined from the tensile strength data of neat foams [15], eq. (4) is applied to predict the filled foam strength, and experimental versus predicted tensile strength values are plotted in

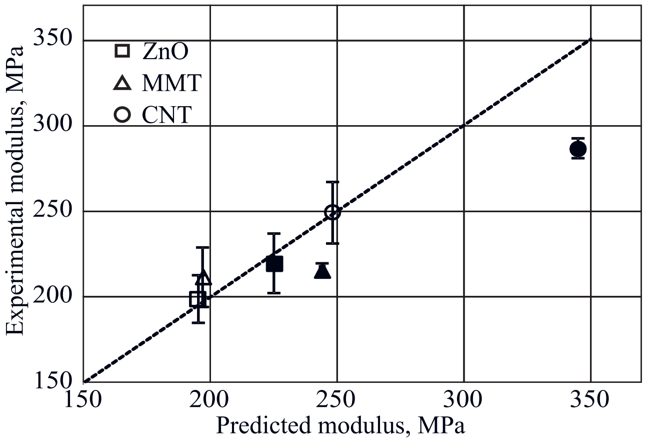

Fig. 6. Experimental strength in the foam rise direction (filled markers, compression) and in transverse direction (open markers, tension) versus the strength predicted by eq. (4) for filled foams with 1 wt % loading of nanoparticles; dashed line corresponds to perfect agreement of prediction and test results

Fig. 6 by open markers. It is seen that the largest reinforcing effect on the foam strength is provided by CNT, as in the case of stiffness. However, it should be noted that the effect of fillers on the foam strength and stiffness is related in part to their influence on the foaming process. That in turn led to density differences of the filled foams: ZnO-, MMT-, and CNT-filled foams had apparent densities of 45 kg/m^3, 46 kg/m^3, and 54 kg/m^3, respectively. The markedly higher density of CNT-filled foams also contributes to the apparent efficiency of reinforcement. The strength values predicted by eq. (4) are reasonably close to the experimental ones, apart from the case of compressive strength of CNT-filled foams, which is overestimated by ca. 17 %.

CONCLUSIONS

Rigid, low-density PIR foams have been developed that incorporate natural oil polyols, synthesized from rapeseed oil. The foam stiffness and strength were shown to be comparable to those of petrochemical origin. Three types of nanoparticles, iso-dimensional (zinc oxide), fibrous (carbon nanotubes), and platelets (organically modified clay) have been applied as fillers of monolithic polymers and foams at 1 wt %. The highest gain in stiffness and strength of composite foams was achieved using CNT. The relative increase in filled foam stiffness and strength was found to be commensurate with that of a monolithic composite.

The research has been funded by the ERDF via project 2010/0290/2DP/2.1.1.1.0/10/APIA/VIAA/053.

REFERENCES

[1] Montero de Espinosa L., Meier M.A.R.: *Eur. Pol. J.* **2011**, *47*, 837.

[2] Stirna U., Fridrihsone A., Lazdina B., Misane M., Vilsone D.: *J. Polym. Environ.* **2013**, *21*, 952.

[3] Lee L.J., Zeng C.H., Cao X., Han X., Shen J., Xu G.: *Compos. Sci. Techn.* **2005**, *65*, 2344.

[4] Ibeh C.C., Bubacz M.: *J. Cell. Plast.* **2008**, *44*, 493.

[5] Saha M.C., Kabir Md.E., Jeelani S.: *Mater. Sci. Eng., A* **2008**, *479*, 213.

[6] Stirna U., Cabulis U., Beverte I.: *J. Cell. Plast.* **2008**, *44*, 139.

[7] Ridha M., Shim V.P.W.: *Exper. Mech.* **2008**, *48*, 763.

[8] Maksimov R.D., Plume E.: *Mech. Compos. Mater.* **2012**, *48*, 487.

[9] Ashby M.F.: *Metall. Trans. A* **1983**, *14*, 1755.

[10] Gibson L.J.: *Mater. Sci. Eng., A* **1989**, *110*, 1.

[11] Gibson L.J., Ashby M.F.: „Cellular solids", Cambridge University Press, Cambridge 1997.

[12] „Mechanics of Cellular Plastics" (Ed. Hilyard N.C.), Macmillan, New York 1982.

[13] Cabulis U., Kirpluks M., Andersons J.: *Key Eng. Mater.* **2013**, *559*, 19.

[14] Zhou J., Allameh S., Soboyejo W.O.: *J. Mater. Sci.* **2005**, *40*, 429.

[15] Andersons J., Cabulis U., Stirna U.: Proceedings of 13th International Conference Fracture, June 16—21, 2013.

Received 29 IV 2013.